Blue-Emitting 2-(2'-Hydroxyphenyl)Benzazole Fluorophores by Modulation of Excited-State Intramolecular Proton Transfer (ESIPT): Spectroscopic Studies and Theoretical Calculations

Maxime Munch,[a] Erika Colombain,[a] Timothée Stoerkler,[a] Pauline M. Vérité,[b] Denis Jacquemin,[b]* Gilles Ulrich,[a]* and Julien Massue [a]*

[a] Institut de Chimie et Procédés pour l'Energie, l'Environnement et la Santé (ICPEES), Equipe Chimie Organique pour la Biologie, les Matériaux et l'Optique (COMBO), UMR CNRS 7515, Ecole Européenne de Chimie, Polymères et Matériaux (ECPM), 25 Rue Becquerel, 67087 Strasbourg Cedex 02, France

[b] CEISAM, UMR CNRS 6230, University of Nantes, Nantes 44322, France.

Emails: Denis.Jacquemin@univ-nantes.fr, gulrich@unistra.fr, massue@unistra.fr,

TOC graphic

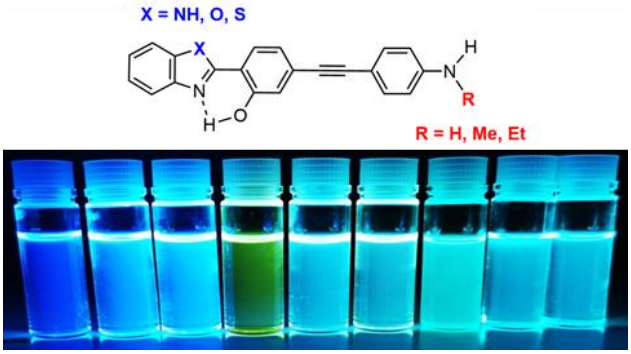

This article describes the synthesis, spectroscopic studies, and theoretical calculations of nine original fluorophores based on the 2-(2'-hydroxyphenyl)benzazole (HBX) scaffold, functionalized at the 4-position of the phenol ring by an ethynyl-extended aniline moieties. HBX dyes are well-known to display Excited-State Intramolecular Proton Transfer (ESIPT) process owing to a strong six-membered hydrogen bond in their structure that allows for an Enol/Keto tautomerism after photoexcitation. Appropriate electronic substitution can perturb the ESIPT process, leading to dual fluorescence, both excited tautomers emitting at specific wavelengths. In the examples described herein, it is demonstrated that the proton transfer can be finely frustrated by a modification of the constitutive heteroring, leading to a single emission band from the excited enol or keto tautomer, or a dual emission with relative intensities highly dependent on the environment. Moreover, the nature of the functionalization of the N-alkylated aniline moiety has also a significant importance on the relative excited state stabilities of the two tautomers in solution. To shed more light on these features, quantum chemical calculations by density functional theory (DFT) are used to determine the excited-state energies and rationalize the experimental spectroscopic data.

Introduction

Organic fluorophores are extensively studied for their low-cost, up-scalability, industrial processability, and possibility to finely tune the emission color upon request. Indeed, fluorescent dyes lie at the crossroad of many innovative applications in the fields of organic electronics, imaging, sensing, encryption data, along with various luminescent displays and materials.[1] Numerous structures and architectures have been reported in efforts aiming to, e.g., improve the stability, tune the photophysical properties, and/or reduce the number of synthetic steps. In this context, Excited-State Intramolecular Proton Transfer (ESIPT)-capable dyes have notably caught the attention of the community.[2,3] ESIPT is a four-level phototautomerization process typically starting from the enol (E) isomer in the ground electronic state, owing to a strong intramolecular 5- or 6-membered hydrogen bond. Upon photoexcitation, proton transfer, from the excited enol (E^*) occurs within the sub-picosecond timescale to yield the excited keto (K^*) tautomer, which decays to the ground-state (K), accompanied by a massive redshift as compared to absorption; the unstable K form rapidly transforming into E to close the cycle (Figure 1). In many dyes, the ESIPT process is guided by the relative excited state energies of the tautomer and, consequently, single K^* emission (when K^* is much more stable) or dual E^*/K^* fluorescence (when K^* is only slightly favored) can be observed experimentally; this equilibrium being very sensitive to both substitution patterns and environment.[4] The latter dual emission process has been notably used to engineer panchromatic white emission from a single dye, a sought-after feature for the construction of white OLED devices.[5-8]

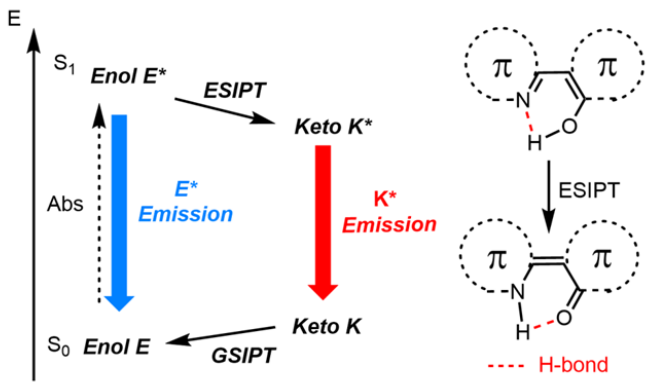

Figure 1. Schematic representation of the four-level phototautomerization process of ESIPT.

One of the main advantages of ESIPT luminescence is its enhanced spectral separation between absorption and emission spectra, leading to large Stokes shifts, up to 10000 cm^{-1},

thereby suppressing self-absorption processes and inner-filter effects and ultimately increasing photostability.[9-11] Furthermore, the proton transfer can be easily perturbed by protic environment or the presence of selected biosubstrates, making these dyes attractive probes for ratiometric chemosensing[12-14] and bioimaging.[15] Various fundamental studies have explored multiple ways to finely tune the optical profiles of ESIPT dyes, such as emission color, fluorescence intensity, excited-state lifetime, as well as proton transfer partial/full frustration, in order to widen the panel of possible applications of ESIPT dyes. Among the many different reported organic scaffold displaying ESIPT,[16-20] 2-(2'-hydroxyphenyl)benzazole (HBX) fluorophores have been widely used as model dyes due to their straightforward synthesis, stability, modularity, biocompatibility, and possibility to control their optical signatures thanks to small structural modifications.[21] For instance, the nature of the heteroatom can be readily modified during the synthesis to provide 2-(2'-hydroxyphenyl)benzoxazole (HBO), 2-(2'-hydroxyphenyl)benzothiazole (HBT) or 2-(2'-hydroxyphenyl)benzimidazole (HBI) derivatives, which induces significant spectral differences. Indeed, HBT dyes show the most redshifted spectra in the series due to the enhanced polarizable nature of the thiazole ring[22-24] whereas HBI derivatives deliver the highest quantum yields (QY),[25] owing to decreased non-radiative deactivations. Meanwhile, the impact of incorporating electrodonors (ED) or electroacceptors (EA) via π-conjugated spacers such as styryl[26] or ethynyl[27-28] at different positions of the HBX scaffold has also been studied leading to a large panel of effects such as apparition of an intramolecular charge transfer (ICT) emission, increase of solution QY, stabilization of anionic species or frustration of the ESIPT process.[22-24,27,28] Recent developments have also highlighted the possibility to engineer dual-state emissive (DSE) dyes based on the HBX scaffold.[29]

In the present article, we aim to provide additional insights into the photophysics of HBX dyes by simultaneously tuning two key parameters reported to modify the E^*/K^* balance, i.e., 1) the nature of the heteroatom (S, O, or N); and 2) the presence of ethynyl-extended ED groups comprised of mono N-alkylated anilines (Me or Et) (Figure 2). A systematic evaluation of the optical properties was done in different solvents, under protonated conditions and in the solid-state, with the view of establishing structure-properties relationships. The photophysical observations were rationalized by DFT calculations.

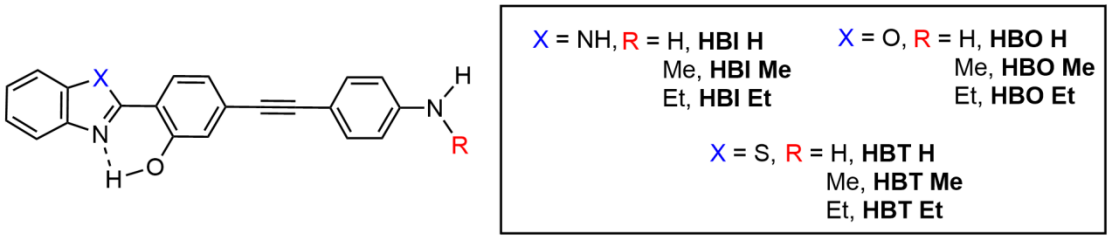

Figure 2. General structure of the HBX-ESIPT dyes studied herein.

Methods

All chemicals were received from commercial sources and used without further purification. Tetrahydrofuran was distilled over sodium. Dichloromethane was distilled over P_2O_5 under an argon atmosphere. ^{1}H NMR and ^{13}C NMR spectra were recorded on a Bruker Advance 400 or 500 MHz spectrometers with perdeuterated solvents. Absorption spectra were recorded using a dual-beam grating Schimadzu UV-3000 absorption spectrometer with a quartz cell of 1 cm of optical path length. The steady-state fluorescence emission and excitation spectra were recorded by using a Horiba S2 Jobin Yvon Fluoromax 4. All fluorescence and excitation spectra were corrected. Solvents for spectroscopy were spectroscopic grade and were used as received. The fluorescence quantum yields (Φ_{exp}) were measured in diluted solution with an absorption value below 0.1 at the excitation wavelength using the following equation:

$$\Phi_{exp} = \Phi_{ref} \frac{I}{I_{ref}} \frac{OD_{ref}}{OD} \frac{\eta^2}{\eta^2_{ref}} \quad (eq\ 1)$$

I is the integral of the corrected emission spectrum, OD is the optical density at the excitation wavelength, and η is the refractive index of the medium. The reference system used was Rhodamine 6G, Φ = 88% in ethanol (λ_{exc} = 488 nm).

For solid-state measurements, KBr (200 mg) and a selected dye (2 mg, *i.e.* 1% wt) were ground together in a mortar. A pellet was subsequently made and the photophysical data recorded (absolute quantum yield using an integration sphere and emission/excitation spectra). Luminescence lifetimes were measured on a Horiba Scientific TCSPC system equipped with a nanoLED 370. Lifetimes were deconvoluted with FS-900 software using a light-scattering solution (LUDOX) for instrument response. The excitation source was a laser diode (λ_{exc} = 320 nm).

Results & Discussion

The syntheses of **HBX H, HBX Me** and **HBX Et** are reported in Schemes S1-S3, respectively. Briefly, **HBX H** was synthesized from Pd-catalyzed Sonogashira cross-coupling reaction between halogenated HBX and 4-ethynylaniline in 20-62% yield. N-alkylated (Me or Et) 4-ethynylanilines were involved in Sonogashira cross-couplings to provide **HBT Me** and **Et**. Due to the moderate synthetic yields, anilines **7** and **8** (see the SI) were obtained by monoalkylation after t-butyloxycarbonyl protection, before being involved in cross-coupling reactions to yield Boc-protected HBX derivatives, followed by deprotection to provide **HBO Me**, **HBO Et**, **HBI Me** and **HBI Et**. All dyes were characterized by ^{1}H and ^{13}C NMR spectroscopy, as well as HR-MS (see the SI).

The photophysical properties of **HBX H, Me**, and **Et** are compiled in Table 1, while the absorption and emission spectra of all dyes in various solvents are presented on Figure 3 (see also the SI for full list of spectra).

HBO H exhibits a main absorption band centered around 365 nm in benzene, dichloromethane (CH_2Cl_2) and ethanol (EtOH) with molar absorption coefficients ranging from 40,500 to 61,000 $M^{-1}.cm^{-1}$. After photoexcitation at 350 nm, a single emission band is observed at 430 nm in benzene with a QY of 62%. A bathochromic shift is observed in CH_2Cl_2 and EtOH where the emission band is moved to 470 and 515 nm, respectively. Going to a polar, protic solvent such as EtOH is accompanied by a marked decrease in QY value, down to 3% correlated with an increase in k_{nr} to $44.1x10^{8}s^{-1}$, one order of magnitude more than in benzene. The strong dependence of the emission wavelength on the dielectric constant of the medium suggests the presence of an ICT-type emission, such as in similar HBO dyes in which the ESIPT process was found to be completely frustrated due to the extension of the conjugation at the 4-position.[26,30] The observed emission can therefore be ascribed to the sole decay of the excited enol state E^{*}. We underline that the amino donor group ($-NH_2$) is logically at the origin of this ICT emission since it is not observed when a methyl group is present instead.[31] As a result of the absence of ESIPT, a bright blue emission is observed in benzene (Figure 3).

Table 1. Photophysical data for **HBX H, Me** and **Et**.

Dye	Solvent	λ_{abs} [a] (nm)	ε [b] ($M^{-1}.cm^{-1}$)	λ_{em} (nm)	$I_{(E^*)} / I_{(K^*)}$	Φ_f [c]	Δ_{ss} [d]	τ (ns)	k_r [e]	k_{nr} [e]
HBO H	Benzene	363	50000	430	1/0	0.62	4300	1.0	6.5	4.0
	CH_2Cl_2	360	61000	470	1/0	0.68	6500	1.5	4.4	2.0
	EtOH	370	40500	515	1/0	0.03	7600	0.2	1.4	44.1
	Solid[f]	435[g]	-	531	[h]	0.01	4200	-	-	-
HBO Me	Benzene	372	51100	438	1/0	0.76	4100	1.1	6.9	2.2
	CH_2Cl_2	372	50500	489	1/0	0.68	6400	2.0	3.4	1.6
	EtOH	379	46300	526	1/0	0.03	7400	0.2	1.3	40.4
	Solid[f]	466[g]	-	532	[h]	0.03	2700	-	-	-
HBO Et	Benzene	374	50600	439	1/0	0.86	4000	1.1	7.6	1.2
	CH_2Cl_2	374	53400	491	1/0	0.76	6400	2.1	3.7	1.2
	EtOH	377	47500	526	1/0	0.04	7500	0.3	1,4	34.3
	Solid[f]	462[g]	-	520	[h]	0.05	2400	-	-	-
HBT H	Benzene	374	57000	430/510	0.12/1	0.18	7100	0.9	2.0	9.3
	CH_2Cl_2	372	53700	509	[h]	0.18	7200	0.9	2.0	9.3
	EtOH	374	44600	517	[h]	0.03	7400	0.2	1.3	40.4
	Solid[f]	446[g]	-	520	[h]	0.01	3200	-	-	-
HBT Me	Benzene	383	49800	453/510	1/0.77	0.20	4000	0.8	2.4	9.6
	CH_2Cl_2	380	45900	513	[h]	0.30	6800	2.0	1.5	3.5
	EtOH	384	48000	533	[h]	0.06	7300	0.3	1.7	26.4
	Solid[f]	461[g]	-	522	[h]	0.01	2500	-	-	-
HBT Et	Benzene	383	43000	452/505	1/0.72	0.19	4000	0.8	2.3	9.6
	CH_2Cl_2	381	53600	515	[h]	0.33	6800	2.2	1.5	3.1
	EtOH	385	55200	535	[h]	0.04	7300	0.3	1.1	27.4
	Solid[f]	448[g]	-	502	[h]	0.01	2400	-	-	-
HBI H	Benzene	360	49200	480	0/1	0.15	5600	0.9	1.6	9.2
	CH_2Cl_2	358	52400	471	0/1	0.15	5500	0.8	1.8	10.4
	EtOH	356	41000	469	0/1	0.17	6800	0.4	4.9	23.7
	Solid[f]	444[g]	-	460/536	0.8/1	0.01	800	-	-	-
HBI Me	Benzene	364	46300	420/480	0.28/1	0.17	3700	0.8	2.3	11.1
	CH_2Cl_2	364	48900	470	[h]	0.36	6200	1.0	3.6	6.5
	EtOH	362	50800	480	[h]	0.09	6800	0.4	2.3	22.8
	Solid[f]	397[g]	-	496	[h]	0.02	5000	-	-	-
HBI Et	Benzene	366	53600	414/477	0.32/1	0.19	3200	0.8	2.4	10.3
	CH_2Cl_2	363	55300	467	[h]	0.41	6100	1.1	3.8	5.5
	EtOH	362	52500	488	[h]	0.10	7100	0.5	2.0	18.0
	Solid[f]	435[g]	-	470	[h]	0.13	1700	-	-	-

[a] Maximum absorption wavelength [b] Absorption coefficient [c] Relative quantum yield determined in solution using Rhodamine 6G as a reference (λ_{exc} = 488 nm, Φ = 0.88 in ethanol), [d] Stokes shift, [e] k_r (10^8 s^{-1}) and k_{nr} (10^8 s^{-1}) were calculated using: $k_r = \Phi_F/\sigma$, $k_{nr} = (1- \Phi_F)/\sigma$ where σ is the lifetime, [f] as embedded in KBr pellet, PLQY calculated as absolute in an integration sphere fitted to a spectrofluorimeter. [g] Excitation wavelength [h] E^* and K^* bands are coalesced.

Analogs **HBO Me** and **HBO Et** show absorption properties very similar to those of **HBO H**, that is, an unstructured absorption band, observed around 375 nm, regardless of the dielectric constant of the solvent, with molar absorption coefficients of 46,300 and 54,300 $M^{-1}.cm^{-1}$. The emission band recorded after photoexcitation at 360 nm is also very sensitive to the dielectric constant of the medium, with bathochromic shifts observed when comparing emissions in benzene (λ_{em} = 438 nm for **HBO Me** and 439 nm for **HBO Et**) and EtOH (λ_{em} =

526 nm for **HBO Me** and **HBO Et**). The QY values go from 76 and 86% in benzene to 3 and 4% in ethanol for **HBO Me** and **HBO E**, respectively. The origin of this emission band is again attributed to the sole presence of the E^* tautomer in the excited-state, owing to a full frustration of ESIPT. As we detail below, this result is fully consistent with theoretical analyses.

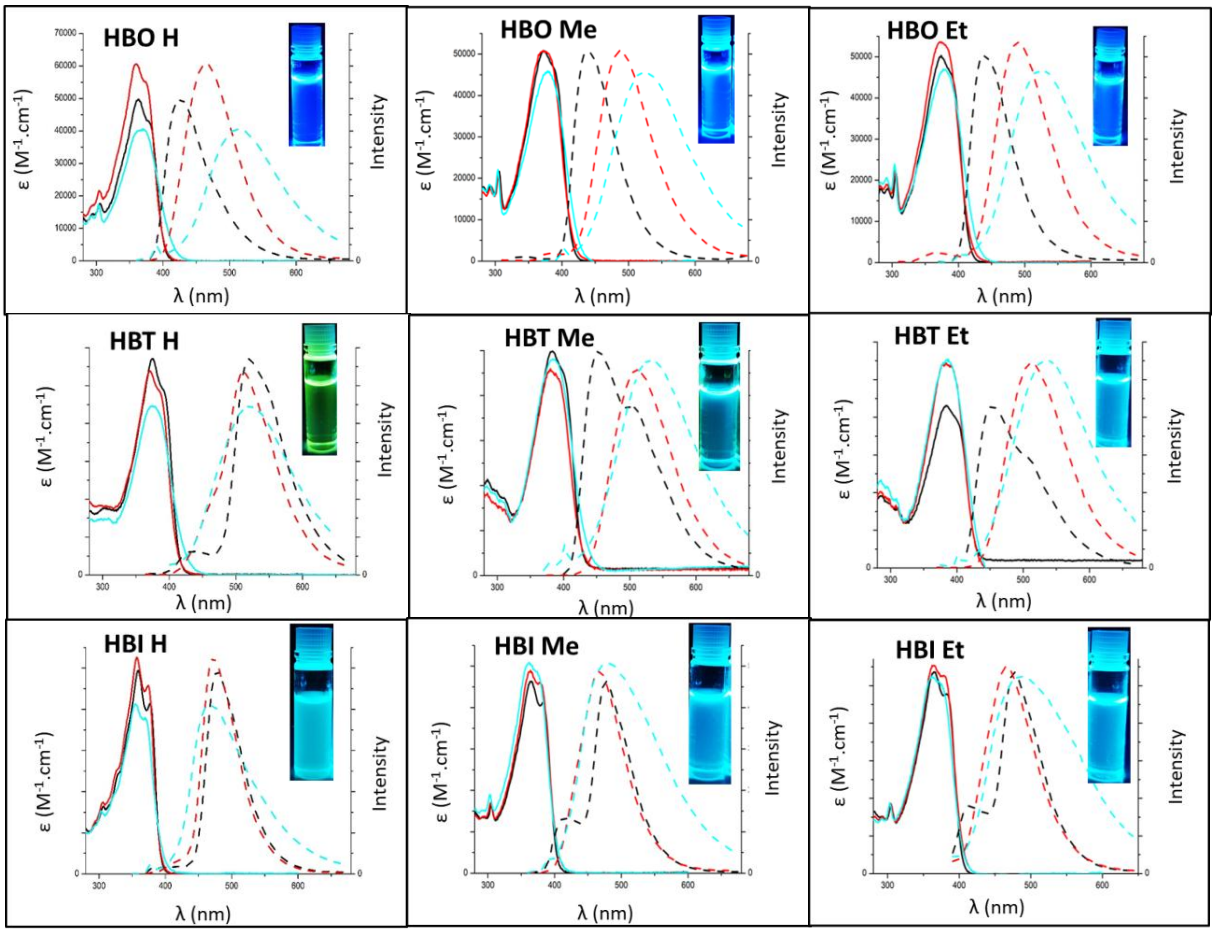

Figure 3. Absorption (plain) and emission (dotted) spectra **of HBX H, Me** and **Et** in benzene (black), CH_2Cl_2 (red) and EtOH (cyan) in aerated solutions at 25°C and (inset) photographs of benzene solutions under irradiation with a bench UV-lamp (λ_{exc} = 365 nm).

HBT H with a NH_2 group, presents an absorption band located at 372-374 nm which is not very sensitive to the polarity of the medium, with molar absorption coefficients in the range 44,600-57,000 $M^{-1}.cm^{-1}$ in benzene, CH_2Cl_2 and EtOH. After excitation at 360 nm, two emission bands are observed in benzene: a weak first one at 432 nm and a more intense second band at 510 nm, respectively attributed to the return to the ground state of the excited E^* and K^* tautomers. This comes in strong contrast with what was observed with **HBO H**, highlighting the marked influence of HBX heteroatom on the stabilization of the first excited-

state. An overall quantum yield of 18% is observed in both benzene and CH_2Cl_2 for **HBT H**. A small bathochromic shift of about 30 nm of the E^* band is observed in the CH_2Cl_2, indicating that E^* is a polar species. In EtOH, a single broad band centered at 517 nm is observed with a QY of 3%. The bathochromic shift as well as the decrease in QY value can be explained by an ICT character of the E^* emission band which coalesces with the K^* band. **HBT Me** and **Et** have absorption spectra similar to that of **HBT H**, exhibiting a single band between 380 and 385 nm (Figure 3), with molar absorption coefficients between 45,900 and 53,600 $M^{-1}.cm^{-1}$. The emission spectra of these compounds in benzene reveal the presence of a band at 453 nm with a marked shoulder at 505 nm attributed to the dual E^*/K^* decay, with QY of 20% and 19% for **HBT Me** and **Et**. The introduction of a single short alkyl group on the nitrogen atom has clearly a strong influence on the of the $I_{(E^*)}/I_{(K^*)}$ ratio (Table 1). The E^* band appears to be much more intense for **HBT Me** and **Et** than for **HBT H**, which is due to the increase in the electron-donating character of the secondary amine vs. primary amine, which does enrich the phenol ring in electron density and diminishes the excited-state acidity of the phenolic proton (that is, increases of pK_a^*). This evolution is clearly seen in the theoretical calculations as well (*vide infra*). A single broad band at 513 nm for both dyes is observed in CH_2Cl_2 with QY of 30% and 33% for **HBT Me** and **Et**. This band is shifted 20 nm towards the low energies in ethanol. The comparison of the optical properties of the three HBT derivatives indicates that the ICT phenomenon is more marked for **HBT Me** and **Et**, consistent with the stronger electron-donating ability of the ED group. At this stage, one can already notice that our examples strikingly illustrate the strong impact on the properties of small structural modifications (S *vs* O, Me *vs* H) on both the stabilization of the E^* state and on the overall photophysical signatures.

Finally, within the HBI series, the **HBI H, Me**, and **Et** dyes all exhibit absorption bands between 360 and 364 nm in benzene with molar absorption coefficients between 41,000 and 55,300 $M^{-1}.cm^{-1}$. As observed in the other series, the influence of solvent or substitution is mild. After photoexcitation at 340 nm, in benzene, a single emission band is observed at 480 nm for **HBI H** with a QY of 15%. In CH_2Cl_2, this emission band is slightly redshifted with a similar QY value, whereas in EtOH, a broad emission band ranging from 400 to 600 nm (λ_{em} (max) = 469 nm, QY = 17%) is recorded. Large Stokes shifts values (between 5500 and 6800 cm^{-1}), combined with a relatively weak dependence of the maximum emission wavelength (absence of ICT) and the QY on the polarity of the medium led us to believe that the emission only stems from K^* state in **HBI H**. However, for **HBI Me** and **HBI Et**, a dual E^*/K^* emission at 420/480 nm and 414/477 nm is observed in benzene with QY of 17 and 19%,

respectively. In CH_2Cl_2, a single K^* band at 470 nm and 467 nm with a QY of 36 and 41% is observed for these alkylated dyes. Compared to benzene, this QY increase correlates with an increase of k_r (2.3 x 10^8 s^{-1} in benzene and 3.6 x 10^8 s^{-1} in CH_2Cl_2 for **HBI Me**) and a decrease in k_{nr} (11.1 x 10^8 s^{-1} in benzene and 6.5 x 10^8 s^{-1} in CH_2Cl_2). The same trend is observed for **HBI Et**. In EtOH, a broad emission band is observed at 480 and 488 nm for **HBI Me** and **Et** as well as a strong decrease in QY at 9 and 10%.

The photophysical behavior of **HBX H, Me**, and **Et** dyes is therefore highly dependent on both structural, that is, the nature of the heteroatom (O, S or N) and aniline monoalkylation (Me or Et), and environmental parameters, namely the polarity and protic nature of the solvent. The combination of these factors allows to finely control the relative energies of the E^* and K^* species, and hence to induce a more or less pronounced proton (back) transfer from E^*(K^*). As a result, single E^*, single K^* or dual E^*/K^* with different intensity ratio can be observed. To further illustrate this aspect, the absorption/emission spectra were superimposed along with the nature of alkylation or nature of heteroatom (Figure 4).

The introduction of an alkyl group (Me or Et) on the amino group on the 4-aminoethynylphenyl group of HBX dyes induces two major changes as compared to the reference primary amine. First evidences indicate a stabilization of the E^* state, owing to a richer electron density on the phenol ring by the presence of an ethynyl-extended secondary amine instead of primary (Figure 4a). This leads to an increase of the pK_a^* of the phenolic proton and a subsequent partial frustration of the ESIPT process. This phenomenon, confirmed by theoretical calculation (*vide infra*), can be observed for **HBT Me, Et** and **HBI Me, Et** derivatives which have a dual E^*/K^* emission in benzene. For **HBO Me** and **Et** dyes, the frustration of the ESIPT process is total and the E^* band at is solely observed. Finally, **HBI H** presents a fluorescence emission stemming almost exclusively from the K^* state at 480 nm, whereas **HBI Me** and **Et** have dual E^*/K^* emissions of relatively similar intensity ratios.

The most striking difference is observed in the HBT series. While **HBT H** exhibits a dual E^*/K^* emission at 433 nm and 510 nm in benzene with relative E^*/K^* intensities of 0.12/1, the introduction of a Me or Et group leads to complete inversion of excited-state prominence (relative E^*/K^* intensities of 1/0.77 and 1/0.72, for **HBT Me** and **HBT Et** respectively) (Figure 4c). Such spectacular spectroscopic outcomes originate from relatively small differences in the relative energies of the two species (*vide infra*); the ESIPT reaction can indeed be viewed as extremely sensitive to perturbations.

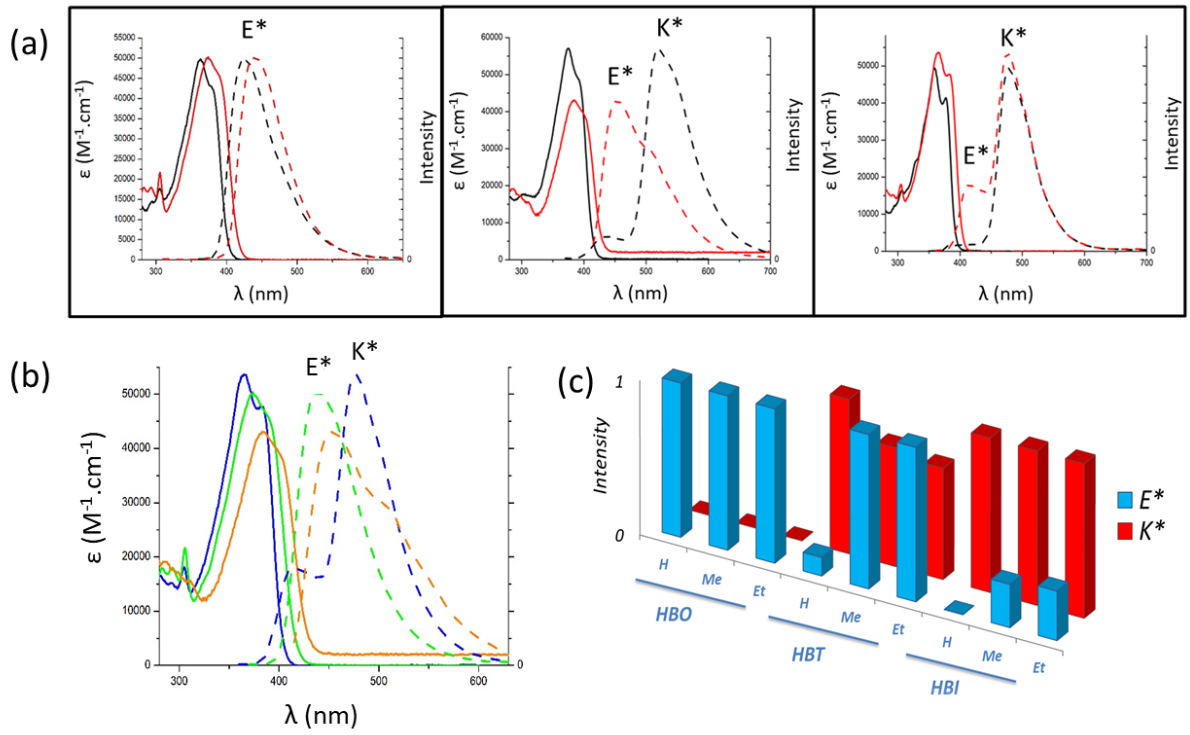

Figure 4. (a) Absorption (plain) and emission (dotted) spectra of **HBO H** (black)/**HBO Et** (red) (left), **HBT H** (black)/**HBT Et** (red) (center) and **HBI H** (black)/**HBI Et** (red) (right) recorded in benzene at 25°C, (b) Absorption (plain) and emission (dotted) spectra of **HBO Et** (green), **HBT Et** (orange) and **HBI Et** (blue) recorded in aerated solutions in benzene at 25°C and (c) Representation of the nature of the emission band(s) for **HBX H, Me** and **Et** in benzene.

A second highlight is the significant increase of the ICT process upon monoalkylation of the aromatic amine with the simplest substituents (Me or Et), induced by the enhanced ED ability of the secondary amines as compared to primary ones. ICT bands are usually strongly influenced by the dielectric constant of the solvent and become more redshifted as the polarity of the environment increases. This feature is particularly marked in the HBT series. The emission of **HBI H** is little impacted by the dielectric constant of the solvent, consistent with a sole K^* emission character, while **HBI Me** or **Et** display significant solvatofluorochromism from 450 to 535 nm when switching from benzene to EtOH. The E^* band being more polarizable than the K^* one, a coalescence is usually observed between both bands in EtOH and only one broad band is observed. It is worth noting that this coalescence process impedes the possibility to accurately attribute the nature of this broad (sole E^* or coalesced E^*/K^*). Again, these trends are confirmed by theoretical modelling.

As for the nature of the heteroatom, significant differences are clearly observed (Figure 4b). The absorption band of **HBI Et** (λ_{abs} = 366 nm) is redshifted to 374 nm and 383 nm for the oxygen and sulfur analogs, namely **HBO Et** and **HBT Et**. The emission also undergoes a bathochromic shift when going from nitrogen to oxygen then to sulfur (λ_{em} = 477 and 505 nm for **HBI Et** and **HBT Et**, respectively). These comparisons are possible in benzene but are difficult in both CH_2Cl_2 and EtOH because of the above-mentioned coalescence of the enol and keto bands. The nature of the heteroatom of the benzazole ring has thus a significant impact on the relative excited-state energies: going from a benzimidazole to a benzoxazole and next to a benzothiazole redshifts the emission wavelengths, as already observed in other examples.[25,32] Owing to the presence of the most electronegative atom in the series, oxygen, the HBO series show the strongest ICT-based emission profile, as evidenced by a strong solvatofluorochromism, even in the case of the primary amine **HBO H**. This is consistent with a full frustration of the ESIPT process. The HBT series exhibit mixed behavior with E^*/K^* emission of various ratios depending on substitution and solvents, while the HBI series have an emission of purely ESIPT nature in benzene (Figure 4).

The **HBX H, Me** and **Et** studied herein all possess an aromatic amino moiety which is easily prone to protonation. Protonation on related HBX species has been reported to have a strong influence on ESIPT occurrence as well as on the relative fluorescence intensities of the two E^*/K^* tautomers.[26] Therefore, **HBX H, Me and Et** have been studied as protonated in EtOH, by simply bubbling HCl gas and the absorption/emission profiles compared to those recorded in neutral EtOH (Figure 5).

Upon protonation of the nitrogen atom of the aniline moieties, strong variations of the absorption and emission spectra are observed, the quantitative effects being dependent not only on substitution but most importantly on the nature of the heteroatom. In the HBO series, protonation triggers a blueshift of both absorption and emission, consistent with a push-pull behavior. Indeed, substitution of a neutral secondary amine by an ammonium group strongly decreases electron density on the π-conjugated scaffold and weakens ICT process, resulting in a less stabilized E^* state. Based on these observations, it is however, difficult to attribute the nature of this emission band, *i.e.* sole E^* or sole K^*. In the HBT and HBI series, different behaviors are observed, highlighting again the importance of the nature of the heterocycle in the photophysical properties.

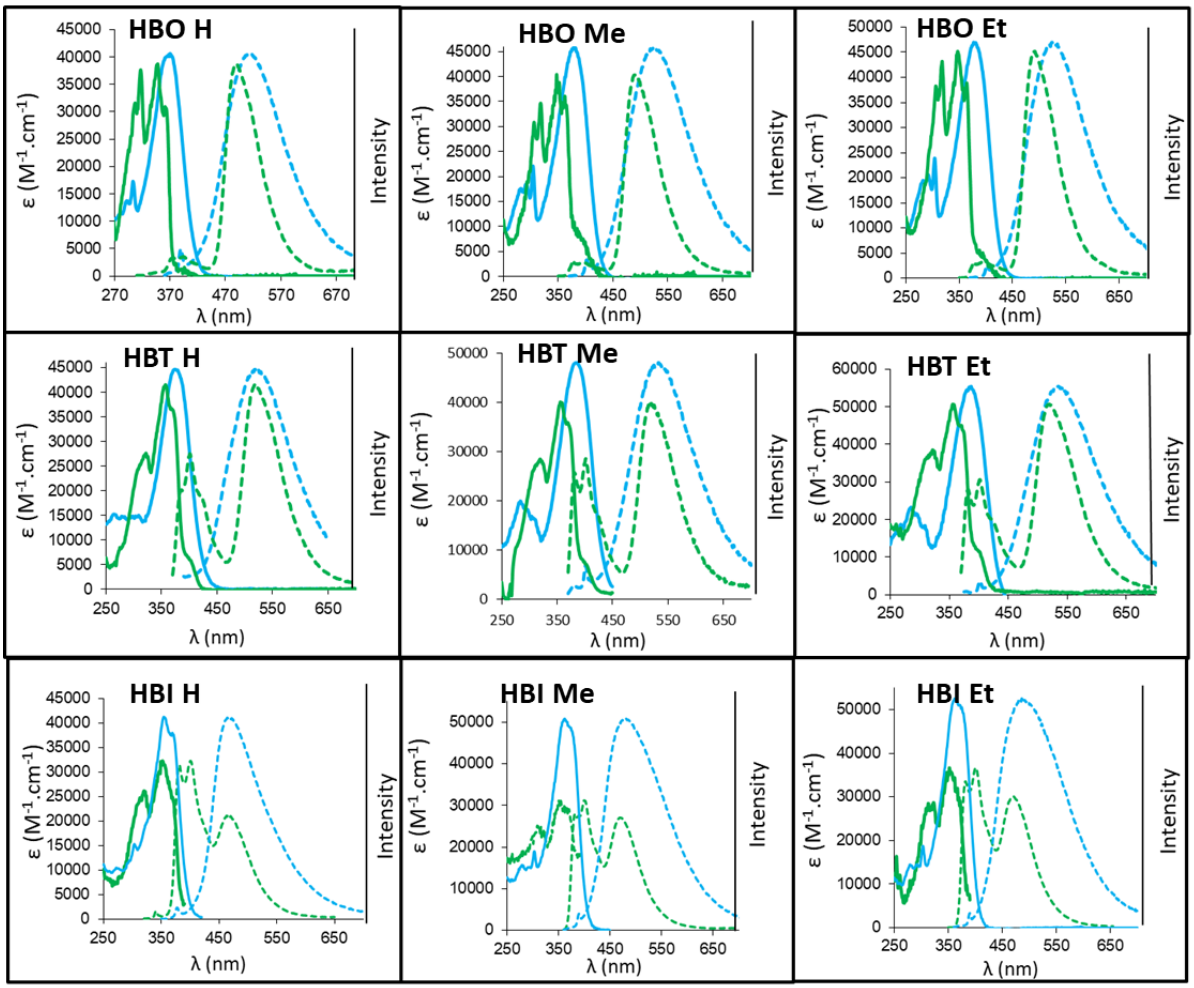

Figure 5. Absorption (plain) and emission (dotted) of **HBX H, Me** and **Et** in EtOH (cyan) and protonated EtOH (green) in aerated solutions at 25°C.

In neutral EtOH, all dyes in these series exhibit a unique broad emission band, due to a coalescence of E^*/K^* bands in protic environment. In all cases, protonation led to the appearance of blueshifted structured absorption band and two emission bands, corresponding to E^* and K^*. The E^* band, of ICT nature, undergoes a significant blueshift upon protonation whereas the K^* band, which does not involve ICT, remains at similar emission wavelength. Protonation thus leads to a more marked spectral separation between the two emission bands.

Finally, the emission of these dyes was studied in the solid-state as embedded in potassium bromide pellets (doped as 1% *wt*). The results are presented on figure 6.

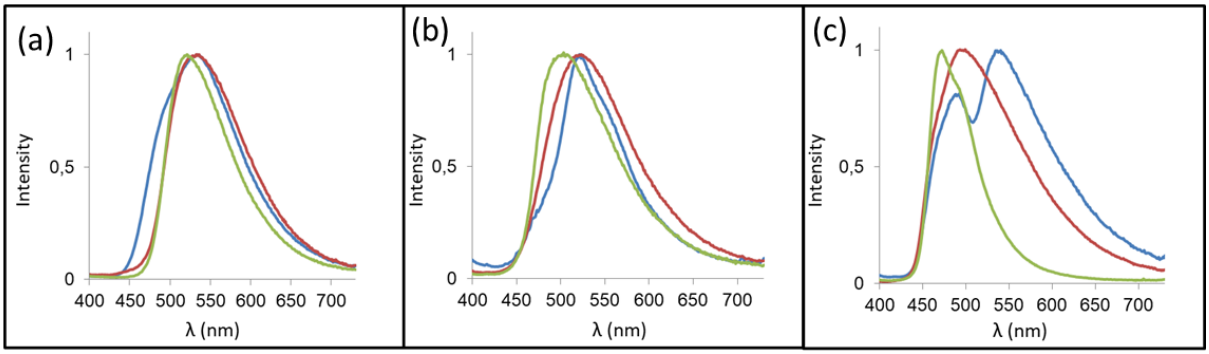

Figure 6. Emission spectra of (a) **HBO H** (blue), **HBO Me** (red) and **HBO Et** (green), (b) **HBT H** (blue), **HBT Me** (red) and **HBT Et** (green) and (c) **HBI H** (blue), **HBI Me** (red) and **HBI Et** (green) as embedded in KBr pellets (1% wt) (concentration around 10^{-5} M).

For the HBO and HBT series, a single broad emission is observed, located between 502 and 532 nm with quantum yields comprised in the 1-5% range. These low QY values, as compared to those usually observed for ESIPT dyes in the solid-state are explained by the prominence of the E^* tautomer leading to aggregation-caused quenching (ACQ) processes. For the HBI series, single or dual emissions are recorded. For **HBI H**, a dual E^*/K^* at 460/536 nm is observed while for **HBI Me** and **HBI Et**, single bands at 496 and 470 nm, respectively are recorded. Considering the strong importance of the environment and substitution on the relative stability of both excited states E^* and K^*, it is presumable that all single broad bands observed in the solid-state arise from a coalescence of both excited tautomers.

To further understand the behavior of the synthesized dyes, we have performed theoretical calculations with a protocol detailed in the SI. In short, all energies are computed with ADC(2)/*aug*-cc-pVTZ, all structures are optimized with TD-DFT and the solvent effects are accounted for using refined continuum solvent model. Such protocol was found very successful for a large panel of HBX ESIPT dyes.[33]

First, we have investigated density difference plots for all compounds (Figures 7 and S63). It can be seen that the amino groups act, as expected, as ED groups as their electronic density decreases upon excitation, whereas the HBX cores act as accepting groups (mostly in red). The ICT character of the transition is clear. Using Le Bahers' metric,[34] the ICT attains 0.54 e (half an electron) over an averaged distance of 3.25 Å for **HBO H**, quite large values, in line with push-pull systems.[35] What is likely more interesting for the ESIPT process is to examine the changes taking place on the hydroxyl and heterocyclic nitrogen atom. For the latter, one notices the usual increase of electronic density, *i.e.*, the group becomes more basic in the

excited state, consistent with a hydrogen-accepting moiety. In contrast, the hydroxyl group is almost unaffected by the transition, that is its acidity is not strongly modified upon excitation as one notices tiny blue lobes. This behavior contrasts with the one found in typical "strong ESIPT" systems,[32,33,36] in which the decrease of density localized in the OH group is much more marked. Going a bit further in the analysis, one notices in Figure 7 that going from the primary to the secondary amines has a deleterious effect on the change of density on the hydroxyl, and that the decreases of density of OH are smaller in the two HBO dyes than in their HBI analogues. Qualitatively, this hints that ESIPT is more likely in **HBI H** than in **HBO Me**. This trend, clearly fitting experimental trends, is further quantified below.

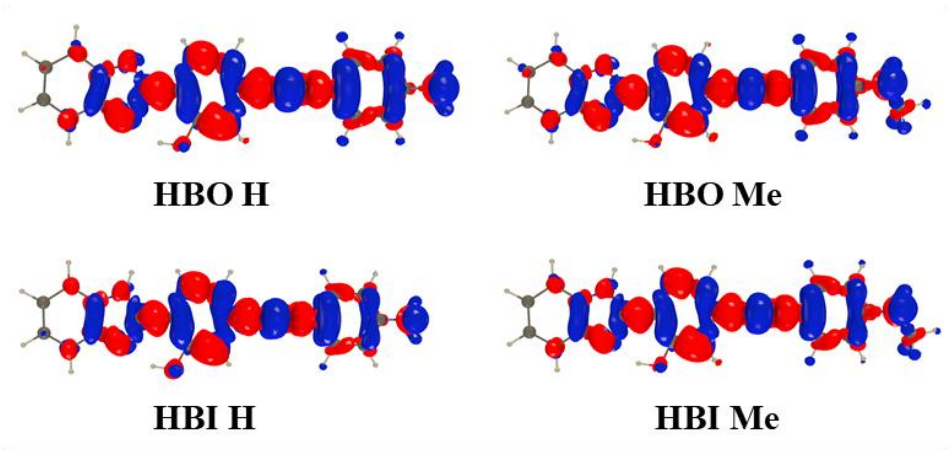

Figure 7. Representation of the differences between the excited and ground state densities computed for **HBO H**, **HBO Me**, **HBI H** and **HBI Me**. The navy blue and crimson red lobes respectively correspond to zones of decrease and increase of density upon photon absorption. Contour threshold: 8 x 10^{-4} au. See also Figure S63.

In Table 2, we report the computed absorption and emission wavelengths, of both E^* and K^* for the latter, as well as the relative excited-state energies of the two tautomers, ΔE. This value is often a good indicator of ESIPT: positive ΔE indicates a more stable enol, and hence, the absence of ESIPT, a strongly negative ΔE hints at quantitative proton transfer, whereas slightly negative ΔE are typical of dual emitters.[33] Before starting our discussion, one should of course issue a word of caution: theoretical simulations are never perfectly accurate, and the accuracy is likely significantly poorer for EtOH, as the used continuum solvation model does not account for solute-solvent H-bonds.

Table 2. Theoretical values. Vertical transition energies are given in nm — all absorption values correspond to the enol form. The relative energies of the excited keto and enol are

given in eV together with the theoretical prediction of emission species according to this energy difference.

Dye	Solvent	λ_{abs}^{vert} (nm)	λ_{em}^{vert} (E*) (nm)	λ_{em}^{vert} (K*) (nm)	ΔE (K*-E*) (eV)	Prediction
HBOH	Benzene	349	419	512	+0.02	E*
	CH_2Cl_2	349	445	503	+0.09	E*
	EtOH	349	454	500	+0.11	E*
	$EtOH+H^+$	330	401	498	-0.07	K* + small E*
HBOMe	Benzene	358	429	510	+0.12	E*
	CH_2Cl_2	361	459	501	+0.19	E*
	EtOH	360	468	497	+0.21	E*
	$EtOH+H^+$	331	401	500	-0.07	K* + small E*
HBOEt	Benzene	358	431	511	+0.13	E*
	CH_2Cl_2	361	460	501	+0.20	E*
	EtOH	360	470	498	+0.23	E*
	$EtOH+H^+$	331	401	501	-0.08	K* + small E*
HBTH	Benzene	363	436	549	-0.11	K* + small E*
	CH_2Cl_2	363	464	538	-0.02	Dual
	EtOH	362	473	534	+0.01	E*
	$EtOH+H^+$	343	416	526	-0.14	K*
HBTMe	Benzene	371	446	547	-0.02	Dual
	CH_2Cl_2	373	477	537	+0.06	E*
	EtOH	372	488	533	+0.09	E*
	$EtOH+H^+$	344	416	528	-0.15	K*
HBTEt	Benzene	372	448	547	-0.01	Dual
	CH_2Cl_2	373	479	537	+0.07	E*
	EtOH	372	489	533	+0.10	E*
	$EtOH+H^+$	344	416	529	-0.16	K*
HBIH	Benzene	344	407	502	-0.14	K*
	CH_2Cl_2	344	426	494	-0.10	K* + small E*
	EtOH	362	431	491	-0.08	K* + small E*
	$EtOH+H^+$	335	412	494	-0.11	K* + small E*
HBIMe	Benzene	351	417	502	-0.05	Dual
	CH_2Cl_2	353	436	493	-0.01	Dual
	EtOH	352	442	490	+0.01	E*
	$EtOH+H^+$	335	412	495	-0.12	K* + small E*
HBIEt	Benzene	351	418	502	0.00	Dual
	CH_2Cl_2	352	438	494	+0.01	E*
	EtOH	352	444	490	+0.02	E*
	$EtOH+H^+$	335	411	496	-0.13	K* + small E*

For absorption, the data listed in Table 2 indicate rather mild variations when changing the solvent, consistent with their experimental counterparts (Table 1). The vertical absorption wavelengths are slightly blueshifted as compared to the experimental λ_{abs}(max), a logical consequence of the neglect of vibronic couplings in the theoretical model. Nevertheless, one notes that all trends are well restored with small redshifts when using secondary amines instead of primary ones, and absorption undergoing bathochromic/hypsochromic displacement when going from a HBO to a HBT/HBI core.

Let us now turn to the emission of the HBO series in benzene. For **HBO H**, one notes that the computed fluorescence for the K^* form, 512 nm, is significantly redshifted compared to experiment (430 nm), whereas the theoretical E^* emission, 419 nm, is slightly blueshifted, which is a first hint that the experimental emission is coming from the enol form, i.e., that ESIPT does not take place. Further, one notices a positive ΔE, indicating a more stable E^*, confirming the absence of driving force for the proton transfer process. When going to CH_2Cl_2, and next, EtOH, the computed K^* emission undergoes moderate blueshifts (negative solvatochromism), whereas the E^* emission significantly redshifts. Comparing to the experimental trends of Table 1, this confirms a sole E^* emission for **HBO H** in these two solvents as well. This is also consistent with the increase of ΔE when going to more polar media. This trend can be understood by the magnitude of the excited state dipole moment, that is much larger for E^* (13.6 D in benzene) than for K^* (3.9 D in benzene), the former presenting a clear ICT nature and being therefore much more sensitive to the polarity than the latter. When turning to both **HBO Me** and **HBO Et**, the above-mentioned trends pertain, though the stronger ED character of the secondary amines leads to an even stronger unstabilization of the keto forms (large positive ΔE in all solvents). In short, consistent with the experimental analysis above, the emission of all HBO derivatives comes from the ICT excited-state of the enol structures.

For **HBT H**, theory foresees a strongly different situation than for **HBO H.** Indeed, there is a large driving force for ESIPT (ΔE = -0.11 eV) in benzene, indicating a dominant K^* emission in a dual emitter.[33] This nicely fits the experimental findings (see Figure 4). The vertical emission wavelengths returned by theory are 436 and 549 nm, estimates that reasonably fit the experimental values of 430 and 510 nm for E^* and K^*, respectively. When going from benzene to CH_2Cl_2, one notices as above a significant (small) redshift (blueshift) of the enol (keto) emission accompanied by a significant reduction of the driving force leading to a dual emission prediction. Experimentally, the two bands coalesce making it impossible to measure an exact E^*/K^* emission ratio. In benzene, going from **HBT H** to both **HBT Me** and **HBT Et** induces a reduction of the ESIPT driving force, with now nearly isoenergetic tautomers in the excited state. Again, this is consistent with the fluorescence bands of E^* and K^* of similar intensities obtained experimentally (see Figures 3 and 4). In CH_2Cl_2 and EtOH, the computed ΔE of both **HBT Me** and **HBT Et** become positive, hinting at a fluorescence originating solely from the E^* structure.

For **HBI H** in benzene, our model delivers emission wavelengths of 407 and 502 nm for E^* and K^*, respectively. The experimental λ_{em} is 480 nm, and the computed enol emission is rather far from the experimental value. In addition, the computed driving force is very large, -0.14 eV, which typically indicates (almost) quantitative ESIPT. In other words, theory predicts K^* fluorescence for **HBI H** in benzene, consistent with experiment (Figure 4). When going to CH_2Cl_2, and next EtOH, the ΔE values remain significantly negative (-0.10 and -0.08 eV) and theory therefore foresees dominant K^* with a small E^* emission that remains unseen experimentally in these solvents. Such small disagreement is just due to the limits of the theoretical model. Interestingly, we note that the experimental λ_{em} of **HBI H** undergoes negative solvatochromism (Table 1) and this trend is consistent with a pure K^* emission (Table 2). When adding one alkyl group on the terminal NH_2 group, the driving force for ESIPT decreases and becomes -0.05 eV and 0.00 eV for **HBI Me** and **HBI Et** in benzene, respectively. Such values correspond to dual emitters, which fits the observation of two clear bands experimentally (Figures 3 and 4). When going to more polar solutions, E^* emission becomes more favored and it is likely than the experimental emission in both **HBI Me** and **HBI Et** are either purely originating from the enol or incorporate a small keto contribution coalesced inside a single band.

Finally, let us turn towards the impact of protonation. Of course, modelling the impact of bubbling HCl in a protic medium is not an easy task for theory, still we expect to recover qualitatively reasonable trends by simply protonating the terminal amino group in the model. As done above, we first examined density difference plots (Figures 8 and S64). As expected, when protonating the amino group, its electron-donating character is lost and the topology of the excited states is now more alike the one of typical ESIPT dyes.[33] For **HBO H**, the ICT character is strongly reduced with a CT distance of 1.39 Å as compared to 3.25 Å for the unprotonated dye. Interestingly also, the decrease of electron density on the hydroxyl is much stronger on the protonated dyes than on their neutral counterparts (compare Figures 7 and 8), hinting at a stronger ESIPT ability.

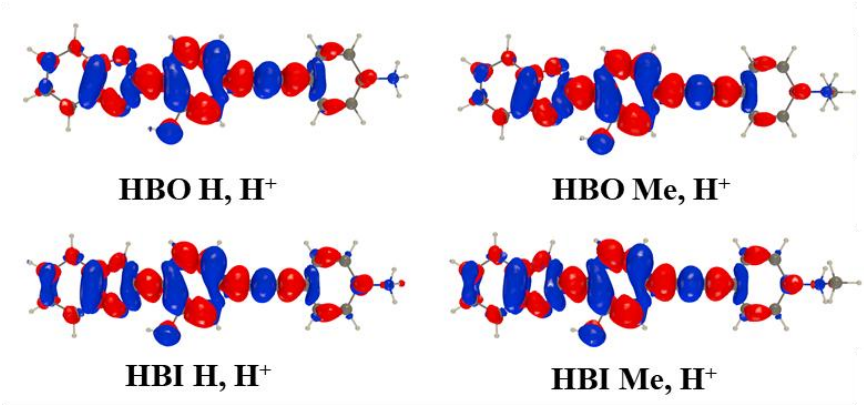

Figure 8. Representation of the difference between the excited and ground state densities computed for selected dyes having their amino group protonated. See caption of Figure 7 for more details. See also Figure S64.

From the data of Table 2, one first notes that the protonation of the amino groups makes the primary and secondary amines essentially equivalent (spectroscopy-wise), so that while the selected heteroatom still impacts the results, the difference between the H, Me, and Et groups are negligible after protonation. This logical trend, also found experimentally (Figure 5), explains why we discuss only the **HBO/HBT/HBI H** cases below. For absorption, protonation yields blueshifts of *ca*. -20 nm according to theory, which clearly fits the experimental trends, at least for the HBO and HBT dyes (Figure 5). For **HBO H** in EtOH, the calculations return a blueshift of -53 nm for the emission of E^* (454 to 401nm), the logical consequence of the strong decrease of the ICT character. In contrast, the K^* emission remains almost unaffected as foreseen (500 to 498 nm). Consistent with Figure 8, one now notes a significant driving force for ESIPT (ΔE = -0.07 eV), hinting at a dominant K^* fluorescence. This is rather consistent with the measurements, which show a strong increase of the Stokes shift when going from neutral to protonated EtOH, though one should likely be cautious for this specific case. For protonated **HBT H**, theory foresees emissions at 416 nm (E^*) and 526 nm (K^*), which fits the experimental spectrum (Figure 5). However, theory predicts a sole emission from the keto species, whereas a dual emission is seen experimentally. It is likely that this disagreement comes from the limitation of continuum models for protic environment. Finally, for **HBI H**, theory predicts a significant yet not very large driving force (ΔE = -0.07 eV) which is compatible with the dual emission observed experimentally.

Conclusion

In conclusion, a series of nine HBX dyes are reported which display a common ethynyl-extended aniline at the 4 position of the phenol ring. Our extended spectroscopic investigations have evidenced that simple monoalkylation of the amino group (Me *vs.* H) has a significant impact on the relative stabilities of the excited states of the two tautomers E^* and K^* and on the subsequent photophysical profiles. The most striking differences come from the nature of the heteroring (O *vs*. S *vs*. N) which can lead either to a quantitative ESIPT process (K^* emission), a dual E^*/K^* emission due to a partial frustration, as well as a complete inhibition of ESIPT (E^* emission). These subtle optical modifications can be further fine-tuned by protonation of the amino residue. First-principle calculations corroborate experimental data in the vast majority of cases, providing precious feedback for the development of future probes. Due to the facile perturbation of the ESIPT process outlined in this article, future developments involve biomolecules chemosensing and bioimaging.

Supporting Information. (^{1}H and ^{13}C NMR spectra, spectroscopic data and details of the computational procedures and methods).

Acknowledgments

The authors are indebted to the ANR for support in the framework of the GeDeMi grant (PhD fellowship for P.M.V.). J.M and G.U. thank the CNRS, the region Grand Est and Amoneta diagnostics for a PhD fellowship for M.M. P.M.V. and D.J. thank the CCIPL (*Centre de Calcul Intensif des Pays de la Loire*) installed in Nantes for generous allocation of computational time. T.S. acknowledges the ministère de l'enseignement supérieur, de la recherche et de l'innovation for a PhD fellowship.

References

(1) de Moliner, F.; Kielland, N.; Lavilla, R.; Vendrell, M. Modern Synthetic Avenues for the Preparation of Functional Fluorophores. *Angew. Chem., Int. Ed*., **2017**, 56, 3758-3769.

(2) Zhao, J.; Ji, S.; Chen, Y.; Guo, H.; Yang, P. Excited state intramolecular proton transfer (ESIPT): from principal photophysics to the development of new chromophores and applications in fluorescent molecular probes and luminescent materials. *Phys. Chem. Chem. Phys*. **2012**, 14, 8803-8817.

(3) Sedgwick, A.C.; Wu, L.; Han, H.-H.; Bull, S.D.; He, X.-P.; James, T.D.; Sessler, J.L.; Tang, B.Z.; Tian, H.; Yoon, J. Excited-state intramolecular proton-transfer (ESIPT) based fluorescence sensors and imaging agents. *Chem. Soc. Rev*., **2018**, 47, 8842-8880.

(4) Massue, J.; Jacquemin, D.; Ulrich, G. Molecular Engineering of Excited-state Intramolecular Proton Transfer (ESIPT) Dual and Triple Emitters. *Chem. Lett*., **2018**, 47, 9, 1083-1089.

(5) Benelhadj, K.; Muzuzu, W.; Massue, J.; Retailleau, P.; Charaf-Eddin, A.; Laurent, A.D.; Jacquemin, D.; Ulrich, G.; Ziessel, R. White Emitters by Tuning the Excited-State Intramolecular Proton-Transfer Fluorescence Emission in 2-(2′-Hydroxybenzofuran)benzoxazole Dyes. *Chem. Eur. J*., **2014**, 20, 12843-12857.

(6) Li, B.; Lan, J.; Wu, D.; You, J. Rhodium(III)-Catalyzed ortho-Heteroarylation of Phenols through Internal Oxidative C-H Activation: Rapid Screening of Single-Molecular White-Light-Emitting Materials. *Angew. Chem., Int. Ed*., **2015**, 54, 14008-14012.

(7) Park, S.; Kwon, J.E.; Kim, S.H.; Seo, J.; Chung, K.; Park, S.-Y.; Jang, D.-J.; Medina, B.M.; Gierschner, J.; Park, S.Y. A White-Light-Emitting Molecule: Frustrated Energy Transfer between Constituent Emitting Centers. *J. Am. Chem. Soc*. **2009**, 131, 14043-14049.

(8) Tang, K.-C.; Chang, M.-J.; Lin, T.-Y.; Pan, H.-A.; Fang, T.-C.; Chen, K.-Y.; Hung, W.-Y.; Hsu, Y.-H.; Chou, P.-T. Fine Tuning the Energetics of Excited-State Intramolecular Proton Transfer (ESIPT): White Light Generation in a Single ESIPT System. *J. Am. Chem. Soc*. **2011**, 133, 17738-17745.

(9) Li, Y.; Dahal, D.; Abeywickrama, C.S.; Pang, Y. Progress in Tuning Emission of the Excited-State Intramolecular Proton Transfer (ESIPT)-Based Fluorescent Probes. *ACS Omega*, **2021**, 6, 6547-6553.

(10) Padalkar, V.S.; Seki, S. Excited-state intramolecular proton-transfer (ESIPT)-inspired solid state emitters. *Chem. Soc. Rev*. **2016**, 45, 169-202.

(11) Berbigier, F.G.; Duarte, L.G.T.A.; Fialho Zawacki, M.; de Araújo, B.B.; de Moura Santos, C.; Atvars, T.D.Z.; Gonçalves, P.F.B.; Petzhold, C.L.; Rodembusch, F.S. ATRP Initiators Based on Proton Transfer Benzazole Dyes: Solid-State Photoactive Polymer with Very Large Stokes Shift. *ACS Appl. Polym. Mater.*, **2020**, 2, 1406-1416.

(12) Zhang, Y.; Yang, H.; Ma, H.; Bian, G.; Zang, Q.; Sun, J.; Zhang, C.; An, Z.; Wang, W.-Y. Excitation Wavelength Dependent Fluorescence of an ESIPT Triazole Derivative for Amine Sensing and Anti-Counterfeiting Applications. *Angew. Chem., Int. Ed*., **2019**, 58, 8773-8778.

(13) Saravana Kumar, P.; Raja Lakshmi, P.; Elango, K.P. An easy to make chemoreceptor for the selective ratiometric fluorescent detection of cyanide in aqueous solution and in food material. *New J. Chem*., **2019**, 43, 675-680.

(14) Sinha, S.; Chowdhury, B.; Ghosh, P. A Highly Sensitive ESIPT-Based Ratiometric Fluorescence Sensor for Selective Detection of Al3+. *Inorg. Chem.*, **2016**, 55, 9212-9220.

(15) Ren, H.; Huo, F.; Wu, X.; Liu, X.; Yin, C. An ESIPT-induced NIR fluorescent probe to visualize mitochondrial sulfur dioxide during oxidative stress in vivo. *Chem. Commun*., **2021**, 57, 655-658.

(16) Stoerkler, T.; Frath, D.; Jacquemin, D.; Massue, J.; Ulrich, G. Dual-State Emissive π-Extended Salicylaldehyde Fluorophores: Synthesis, Photophysical Properties and First-Principle Calculations. *Eur. J. Org. Chem*., **2021**, 26, 3726-3736.

(17) Gobel, D.; Duvinage, D.; Stauch, T.; Nachtsheim, B.J. Nitrile-substituted 2-(oxazolinyl)-phenols: minimalistic excited-state intramolecular proton transfer (ESIPT)-based fluorophores. *J. Mater. Chem. C*, **2020**, 8, 9213-9225.

(18) Mutai, T.; Muramatsu, T.; Yoshikawa, I.; Houjou, H.; Ogura, M. Development of Imidazo[1,2-a]pyridine Derivatives with an Intramolecular Hydrogen-Bonded Seven-Membered Ring Exhibiting Bright ESIPT Luminescence in the Solid State. *Org. Lett*., **2019**, 21, 2143-2146.

(19) Tseng, H.-W.; Lin, T.-C.; Chen, C.-L.; Lin, T.-C.; Chen, Y.-A.; Liu, J.-Q.; Hung, C.-H.; Chao, C.-M.; Liu, K.-M.; Chou, P.-T. A new class of N–H proton transfer molecules: wide tautomer emission tuning from 590 nm to 770 nm via a facile, single site amino derivatization in 10-aminobenzo[h]quinolone. *Chem. Commun*., **2015**, 51, 16099-16102.

(20) Zhang, M.; Cheng, R.; Lan, J.; Zhang, H.; Yan, L.; Pu, X.; Huang, Z.; Wu, D.; You, J. Oxidative C-H/C-H Cross-Coupling of [1,2,4]Triazolo[1,5- a]pyrimidines with Indoles and Pyrroles: Discovering Excited-State Intramolecular Proton Transfer (ESIPT) Fluorophores. *Org. Lett*., **2019**, 21, 4058-4062.

(21) Mishra, V.R.; Ghanavatkar, C.W.; Sekar, N. Towards NIR-Active Hydroxybenzazole (HBX)-Based ESIPT Motifs: A Recent Research Trend. *ChemSelect*, **2020**, 5, 2103-2113.

(22) Ren, Y.; Fan, D.; Ying H.; Li, X. Rational design of the benzothiazole-based fluorescent scaffold for tunable emission. *Tetrahedron Lett.*, **2019**, 60, 1060-1065.

(23) Chen, Y.; Fang, Y.; Gu, H.; Qiang, J.; Li, H.; Fan, J.; Cao, J.; Wang, F.; Lu, S.; Chen, X. Color-Tunable and ESIPT-Inspired Solid Fluorophores Based on Benzothiazole Derivatives: Aggregation-Induced Emission, Strong Solvatochromic Effect, and White Light Emission. *ACS Appl. Mater. Interfaces*, **2020**, 12, 55094-55106.

(24) Niu, Y.; Wang, Q.; Wu, H.; Wanga, Y.; Zhang, Y. Experimental and DFT studies of disubstituted 2-(2-hydroxyphenyl)benzothiazole-based fluorophores synthesized by Suzuki coupling. *New J. Chem*., **2017**, 41, 9796-9805.

(25) Pariat, T.; Munch, M.; Durko-Maciag, M.; Mysliwiec, J.; Retailleau, P.; Vérité, P. M.; Jacquemin, D.; Massue, J.; Ulrich, G. Impact of Heteroatom Substitution on Dual-State Emissive Rigidified 2-(2'-hydroxyphenyl)benzazole Dyes: Towards Ultra-Bright ESIPT Fluorophores. *Chem. Eur. J.,* **2021***,* 27, 10, 3483-3495.

(26) Raoui, M.; Massue, J.; Azarias, C.; Jacquemin, D.; Ulrich, G. Highly fluorescent extended 2-(2′-hydroxyphenyl)benzazole dyes: synthesis, optical properties and first-principle calculations. *Chem. Commun*. **2016**, 52, 9216-9219.

(27) Massue, J.; Ulrich, G.; Ziessel, R. Effect of 3,5-Disubstitution on the Optical Properties of Luminescent 2-(2′-Hydroxyphenyl)benzoxazoles and Their Borate Complexes. *Eur. J. Org. Chem*., **2013**, 5701-5709.

(28) Massue, J.; Felouat, A.; Curtil, M.; Vérité, P.M.; Jacquemin, D.; Ulrich, G. Solution and solid-state Excited-State Intramolecular Proton Transfer (ESIPT) emitters incorporating Bis-triethyl-or triphenylsilylethynyl units. *Dyes Pigm.*, **2019**, 160, 915-922.

(29) Pariat, T.; Stoerkler, T.; Diguet, C.; Laurent, A.D.; Jacquemin, D.; Ulrich, G.; Massue, J. Dual Solution-/Solid-State Emissive Excited-State Intramolecular Proton Transfer (ESIPT) Dyes: A Combined Experimental and Theoretical Approach. *J. Org. Chem.,* **2021**, 86, 17606-17619.

(30) Wang, Q.; Xu, L.; Niu, Y.; Wang, Y.; Yuan, M.-S.; Zhang, Y. Excited State Intramolecular Proton Transfer in Ethynyl-Extended Regioisomers of 2-(2'-Hydroxyphenyl)benzothiazole: Effects of the Position and Electronic Nature of Substituent Groups. *Chem. Asian J.*, **2016**, 11, 3454-3464.

(31) Munch, M.; Curtil, M.; Vérité, P.M.; Jacquemin, D.; Massue, J.; Ulrich, G. Ethynyl-Tolyl Extended 2-(2′-Hydroxyphenyl)benzoxazole Dyes: Solution and Solid-state Excited-State Intramolecular Proton Transfer (ESIPT) Emitters. *Eur. J. Org. Chem*., **2019**, 1134-1144.

(32) Heyer, E.; Benelhadj, K.; Budzák, S.; Jacquemin, D.; Massue, J.; Ulrich, G. On the Fine-Tuning of the Excited-State Intramolecular Proton Transfer (ESIPT) Process in 2-(2′-Hydroxybenzofuran)benzazole (HBBX) Dyes. *Chem. Eur. J*. **2017**, 23, 7324-7336.

(33) Azarias, C.; Budzak, S.; Laurent, A. D.; Ulrich, G.; Jacquemin, D. Tuning ESIPT fluorophores into dual emitters. *Chem. Sci*. **2016**, 7, 3763-3774.

(34) Le Bahers, T.; Adamo, C.; Ciofini, I. A Qualitative Index of Spatial Extent in Charge-Transfer Excitations. *J. Chem. Theory Comput.* **2011**, *7*, 2498-2506.

(35) Ciofini, I.; Le Bahers, T.; Adamo, C.; Odobel, F.; Jacquemin D. Through-Space Charge Transfer in Rod-Like Molecules: Lessons from Theory. *J. Phys. Chem. C.* **2012**, *116*, 11946-11955. Err**:** *ibidem* 14736.

(36) Vérité, P. M.; Guido, C. A.; Jacquemin D. First-principles investigation of the double ESIPT process in a thiophene-based dye. *Phys. Chem. Chem.. Phys.* **2019**, *21*, 2307-2317.